

# The Impact of Microwave-Assisted Thermal Sterilization on the Morphology, Free Volume, and Gas Barrier Properties of Multilayer Polymeric Films

Sumeet Dhawan,<sup>1</sup> Christopher Varney,<sup>2</sup> Gustavo V. Barbosa-Cánovas,<sup>1</sup> Juming Tang,<sup>1</sup> Farida Selim,<sup>2</sup> Shyam S. Sablani<sup>1</sup>

<sup>1</sup>Department of Biological Systems Engineering, Washington State University, Pullman, Washington 99164-6120

<sup>2</sup>Department of Physics and Astronomy, Washington State University, Pullman, Washington 99164-6376

Correspondence to: S. S. Sablani (E-mail: ssablani@wsu.edu)

**ABSTRACT:** Microwave-assisted thermal sterilization (MATS) is an advanced thermal process that utilizes microwave (MW) energy for in-package food sterilization. Benefits include much shorter processing times than conventional retort sterilization. This research explores how MATS affects the performance of high-barrier multilayer polymeric films compared with conventional retort sterilization. The gas barrier, morphological, and free volume packaging properties of these films may influence the shelf-life of shelf-stable foods. In this study, we applied X-ray diffraction (XRD) and positron annihilation lifetime spectroscopy in order to investigate film morphology and free volume characteristics, respectively. Results show that the conventional retort process affected gas barrier properties more than MATS processing did which could be explained by the morphological and free volume changes in the polymeric films. XRD revealed improved crystalline morphology of MW-treated films in terms of overall crystallinity as compared with retort sterilization. On the other hand, higher free volume increase in MW-treated films could be explained by the different heating mechanisms involved in MATS and retort sterilization. Overall, the oxygen transmission rate for both films remained below 2 cc/m<sup>2</sup>-day after MATS and retort sterilization required for packaging applications for shelf-stable foods. This work provides the basis for understanding the gas-barrier changes of multilayer polymeric films after MATS application using Materials Science techniques. © 2014 Wiley Periodicals, Inc. *J. Appl. Polym. Sci.* 2014, 131, 40376.

**KEYWORDS:** X-ray; morphology; differential scanning calorimetry (DSC)

Received 13 June 2013; accepted 31 December 2013

DOI: 10.1002/app.40376

## INTRODUCTION

Consumers' desire for safe, high-quality foods, along with food processors' quest for more energy-efficient, high-throughput, cost-effective processing technologies highlight the need for more advanced food processing technologies.<sup>1</sup> Microwave (MW) heating is purported to be one of the most promising preservation technologies, predicted to dominate the 21st century in terms of the production of shelf-stable foods.<sup>2,3</sup> The reduced processing times in MW heating compared with conventional heating set the stage for the development of high-quality, nutritious, shelf-stable food products.<sup>4</sup> Sterilization of in-packaged foods using MW systems has been commercialized in Europe and Japan.<sup>5</sup> In the United States, a 915-MHz, single-mode and semi-continuous microwave-assisted thermal sterilization (MATS) system for processing low-acid, in-packaged foods was developed by the advanced thermal processing research team at Washington State University.<sup>6</sup> A petition filed

by the same research team to preserve a homogenous low-acid food using the MATS system received U.S. Food and Drug Administration acceptance in October, 2009.

The MATS process requires that food be processed inside its packaging. Metal-based, flexible, meal ready-to-eat (MRE) pouches containing aluminum (Al) foil have been widely used for retort sterilization. However, the Al layers in the MRE pouches shield electromagnetic fields from reaching food in packages and are therefore not suitable for the MATS process. Alternatively, high gas-barrier, polymeric-based packaging materials appear to be viable candidates for advanced thermal sterilization processes. In addition, there is an urgent need to develop suitable packaging materials to extend the shelf-life of MATS-processed food and maximize the advantages of this advanced thermal technology.<sup>7</sup> Therefore, this study fills an important gap in the literature by investigating the interaction between packaging material and MATS food-processing technology.

Most polymeric packaging materials used with advanced thermal food processing technologies consist of more than one polymeric layer. Multilayer polymeric films usually have a core functional barrier layer (a polymer layer responsible for gas barrier properties) that provides the necessary shelf-life for packaged foods. Ethylene-vinyl alcohol (EVOH), poly(ethylene terephthalate) (PET), nylon (Ny), and poly(vinylidene chloride) are functional gas-barrier layers commonly used for packaging shelf-stable foods. Silicon (Si) and aluminum (Al) metal-oxide coated high-barrier multilayer polymeric films, as well as nanoparticle-coated gas barrier layers in multilayer polymeric films have been developed to improve gas barrier properties and are commercially available for retort sterilization treatment.

Few studies have examined the influence of MATS on polymeric-based packaging material. One such study by Mokwena et al.<sup>8</sup> explored the effect of retort and MW sterilization on two multilayer EVOH-based multilayer polymeric lid-stocks for low-acid model food packaged in polymeric trays. Both thermal sterilization technologies resulted in the deterioration of the oxygen barrier of the two films. However, oxygen barrier deterioration was higher in retort sterilization compared with MW sterilization, as the longer processing times of retort sterilization resulted in increasing the plasticization of the hydrophilic EVOH layer, leading to an increased oxygen barrier deterioration.<sup>8</sup> Our study builds on previous research by evaluating the impact of MATS on two new multilayer PET-based packaging materials in order to elucidate the influence of free volume characteristics and film morphology on gas-barrier properties of MATS-processed PET films.

The morphology of a polymer refers to the distribution and homogeneity of crystalline, as well as the amorphous regions within the matrix of the polymer material; it also describes the polymeric chain arrangements. A higher overall crystallinity increases the order of the polymeric chains and reduces void spaces within the polymer matrix, thus leading to better gas barrier properties.<sup>9</sup> The degree of crystallinity of a polymer is determined through the fingerprinting X-ray diffraction (XRD) technique. An inefficient chain packing of the polymer creates free volume, the size, and distribution of which control the rate of gas diffusion and the permeation properties. Positron annihilation lifetime spectroscopy (PALS) can detect the free volume properties of a polymer because positronium (the bound state of positron and electron,  $P_2$ ) are formed and localized in low electron density sites, such as free volumes, interface, and pores.<sup>10</sup> The shape and size of the free volume in the polymer directly affect gas permeation properties.<sup>11,12</sup> However, to date, no known experimental research has linked morphological and free volume property changes in MW processed polymeric multilayer films to gas barrier characteristics. Studies of this nature will help in selecting the right packaging material for the sterilization application and also provide fundamental understanding for the polymer industry to further improve the barrier properties of polymeric packaging materials.

Thus, our objectives are to investigate the influence of MATS on the oxygen transmission rate (OTR) of two multilayer polymeric pouches, one of which is coated with a special barrier layer. In this study, we evaluate post-processing films in order

to understand how free volume characteristics and film morphology affect the gas-barrier properties of MATS processed PET films compared with conventional retorting.

## MATERIALS AND METHODS

### Polymeric Film Composition

Two multilayer polymeric films consisting of PET as the functional barrier layer were subjected to MATS and retort sterilization. Film A was developed by Alcan Packaging (Chicago, IL) and consisted of an outer layer of 15- $\mu\text{m}$ -thick PET, a middle layer of 15  $\mu\text{m}$  of Ny 6, and an inner layer of 50  $\mu\text{m}$  of sealant polypropylene (PP). Film A is denoted as PET/adhesive/Nylon 6/adhesive/PP. Film B was developed by Kuraray Co. (Houston, TX) and had a 12- $\mu\text{m}$ -thick functional barrier layer, PET, with a special barrier coating on either side. The middle layer of film B was a 15- $\mu\text{m}$ -thick oriented-nylon 6 and an inner layer of 50  $\mu\text{m}$  of PP. Film B is denoted as Coated-PET-Coated/adhesive/oriented-Nylon 6/adhesive/PP. The coating on the PET layer in film B used a proprietary barrier technology and contained both organic and inorganic barrier particles to increase the tortuosity of gas flow through the polymer matrix. Flexible pouches of dimension 18 cm  $\times$  12 cm were made from the above two multilayer films. They were filled with 225 g mashed potatoes (a model low-acid food), which were prepared by mixing 15% instant mashed potato flakes (Washington Potato Company, Warden, WA) with 85% deionized water. Pouches were vacuum sealed with minimum head space before thermal sterilization.

### MATS and Retort Treatment

Thermal treatments were applied in a pilot scale 915-MHz, single-mode, semi-continuous MATS system developed at Washington State University.<sup>6</sup> This system consisted of four pressurized sections, namely, preheating, MW heating, holding, and cooling, arranged in series to simulate the four sequential industrial processing steps. Water at a controlled temperature was filled in each section from an individual water circulating system. During processing, the sealed food pouches were loaded on a pocketed mesh conveyor belt which transports them through the different sections of MATS. The preheating section, which included a preheating cavity and a water circulating system, helped equilibrate the food to a uniform initial temperature. Pressurized water at 35 psig and 72°C was supplied to the preheating cavity by a water circulation system, the temperature of which was controlled by resistance temperature detectors (RTD). Pouches in the conveyor were navigated through the MW heating section, which included four single-mode MW heating cavities, four MW generators with a labeled operating frequency at 915 MHz, MW waveguides, and pressurized hot water (35 psig, 124°C) supplied to each of the four cavities through a water circulation system. The MW generators supplied a maximum power of 10, 10, 5, and 5 kW to cavities 1, 2, 3, and 4, respectively. Food in the MW heating section was heated simultaneously with MW energy infringing from the four cavities and by circulating hot water (35 psig, 122°C) through convection/conduction surface heating. The holding section, comprised of the holding cavity, was an extension of the heating system without the MW energy, in which the food

achieves required thermal lethality. Hot water (35 psig, 123°C) was supplied to the holding cavity through the water circulation system. The water temperature in the heating and holding sections was controlled using a RTD sensor similar to the preheating section. Food pouches were finally cooled down to room temperature in the cavity of the cooling section using a cold water circulation system. The forwarded power to and reflected power from each of the four MW-heating cavity were measured by two-directional couplers installed in each of the cavities. Operational parameters were recorded and monitored by the control and data acquisition system present in the MATS system.

Retort sterilization was also carried out in the same unit without turning on the MW generators. In these test runs, the MATS system functioned as a hot water immersion still retort in the absence of application of MW power to the system. Temperature measurements were obtained using Ellab sensors (Ellab, Centennial, CO) at the cold spot of the polymeric pouches. Cold spots were identified using a chemical marker-based computer vision system described in Pandit et al.<sup>13</sup> The procedure for the thermal treatment was selected based on its ability to achieve a similar level of sterilization ( $F_0 = 6$  min) for both retort and MW sterilization. The general method was used to calculate the  $F_0$  values at the cold spot,<sup>14</sup>

$$F = \int_0^t 10^{\left(\frac{T - T_R}{z}\right)} dt \quad (1)$$

where  $T$  is the measured temperature at the cold spot of the product (°C);  $T_R$  is the reference temperature (121.1°C);  $z$  is the temperature rise required to decrease the thermal death time of the target microorganism (*Clostridium botulinum*) by one log cycle (10°C); and  $t$  is the heating time (minutes). Figure 1 shows the representative time-temperature profiles at the cold spot of the polymeric pouches for both MATS and retort sterilization treatment.

#### Oxygen Transmission Rate

A Mocon Ox-Tran 2/21 MH permeability instrument (Modern Control, Minneapolis, MN) was used to conduct OTR measurements. Testing conditions were set at  $55 \pm 1\%$  relative humidity, 23°C, and 1 atm. The test was conducted according to the ASTM standard D 3985 method,<sup>15</sup> and measurements were conducted with a coulometric sensor fitted to the equipment. Film specimens of surface area 50 cm<sup>2</sup> were cut from the polymeric pouches and mounted inside the testing chambers. The OTR of the control (untreated) and MATS processed pouches were measured in replicates.

#### Water Vapor Transmission Rate

A Mocon Permatran 3/33 tester (Modern Control, Minneapolis, MN) was used to characterize the water vapor transmission rate (WVTR) of the packaging materials at 100% RH and 38°C, according to the ASTM standard method F 372-99.<sup>16</sup> This equipment uses an infrared detector to analyze the transmission rates. Film specimens of surface area 50 cm<sup>2</sup> were cut from the polymeric pouches and mounted inside the testing chambers. The WVTR of the control (untreated) and MATS-processed pouches were measured in replicates.

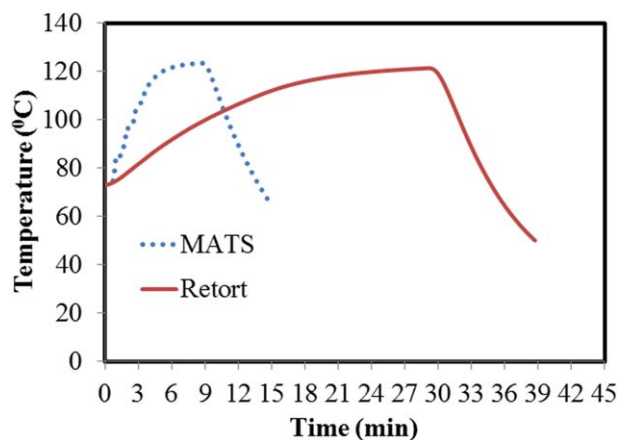


**Figure 1.** Representative temperature and time profile for the cold spot of mashed potato in polymeric pouches during MATS and retort sterilization ( $F_0 = 6$  min). [Color figure can be viewed in the online issue, which is available at [wileyonlinelibrary.com](http://wileyonlinelibrary.com).]

#### Thermal Analysis

A model Q2000 TA Instruments differential scanning calorimeter (DSC) (New Castle, DE) was used to analyze the effect of MATS and retort sterilization on the thermal transitions of films A and B. Film samples weighing  $2 \pm 0.2$  mg were placed in pans and heated from 20 to 300°C at a rate of 10°C/min in the DSC instrument. The resulting DSC thermograms were analyzed to determine the melting temperature ( $T_m$ , °C) and the enthalpy of melting ( $\Delta H$ , J/g) of the polymers present in the multilayer films A and B. The peak temperature of the endotherm corresponds to the  $T_m$  and the  $\Delta H$  was determined by integrating the respective temperature versus the heat flow melting endotherm using the instrument's software. All measurements were conducted in replicates.

#### X-ray Diffraction

X-ray diffractograms for the films before and after thermal sterilization treatments were obtained using a Siemens D-500 diffractometer (Bruker, Karlsruhe, Germany). The X-ray copper target tube was set at 35 kV and 30 mA and operated at a wavelength of 0.15 nm. The sample size of the films was 2 inches  $\times$  2 inches, and the diffraction intensity was recorded as a function of increasing scattering angle from 8 to 35 degrees, with a step angle of 0.05 degrees and a scan time of 3 s per step. The ratio of area under the peaks (crystalline region) to the area of the amorphous region in the diffraction patterns helped estimate the overall crystallinity. The overall percentage of film crystallinity was determined from XRD patterns using the instrument's software.

#### Positron Annihilation Lifetime Spectroscopy

Positron lifetime spectroscopy is a highly informative technique for microscopic characterization of vacancy-type defects in crystals and open volumes in polymers. Positrons injected into a solid from a radioactive source annihilate with electrons, either from a delocalized state in the bulk or from a trapped state in an open volume such as a lattice vacancy in crystals or an open volume in polymers and porous materials. Trapping at defects or open volumes leads to an increase in the average positron

lifetime. In fair approximation, the positron lifetime varies inversely with the electron density at the annihilation site. Consequently, annihilations in vacancies or open volumes, where electron densities are low, have longer lifetimes. Measured lifetimes are characteristic of the open volume in which the positrons annihilate, and therefore, can be used to discriminate among different locations where positrons annihilate. A measured lifetime spectrum  $N(t)$  consists of a sum of components corresponding to each annihilation site<sup>17</sup>:

$$N(t) = \sum_{i=1}^{k+1} \frac{I_i}{\tau_i} \exp\left(-\frac{t}{\tau_i}\right) \quad (2)$$

in which  $k + 1$  is the number of lifetime components in the spectrum, corresponding to annihilation in the bulk and in  $k$  defect types, and in which  $\tau_i$  and  $I_i$  are the lifetime and intensity of the  $i$ th component in the spectrum. Fitted lifetimes give information on defect/open volume sizes and characteristics, whereas intensities determine defect/open volume concentrations. Therefore, the lifetime spectrum provides information on free volumes in polymers and porous materials. Positrons also form positronium in polymers, resulting in a much longer positron lifetime.<sup>10</sup>

Here, positron lifetimes were measured using a conventional fast-fast time coincidence spectrometer with two BaF<sub>2</sub> gamma-ray detectors mounted on photomultiplier tubes.<sup>18</sup> A positron source was made by depositing <sup>22</sup>NaCl activity on an 8- $\mu$ m-thick kapton foil that was then folded and sandwiched between two identical samples. PAL spectra were recorded at room temperature with a time resolution of 250 ps. Several million counts were accumulated in each lifetime spectrum for good statistical precision. The LT9 program was used to analyze the lifetime distribution after applying the source correction term.<sup>19</sup> The measured spectra were resolved into three components ( $\tau_1$ ,  $\tau_2$ , and  $\tau_3$ ) with their respective intensities ( $I_1$ ,  $I_2$ , and  $I_3$ ) for finite-term lifetime analysis. Spectra were fit to the best  $\chi^2$  with the most reasonable standard deviation.

The shortest positron lifetime ( $\tau_1$ ) was attributed to the self-annihilation of para-positronium (p-Ps), whereas the intermediate lifetime ( $\tau_2$ ) was attributed to free positron annihilation. The third mean lifetime ( $\tau_3$ ) was attributed to the ortho-positronium (o-Ps) pick-off annihilation in free-volume holes of the amorphous region. A semi-empirical equation given by the following relation along with the o-Ps lifetime ( $\tau_3$ ) could be used to obtain the mean free-volume hole radius ( $R$ ):

$$(\tau_3)^{-1} = 2 \left[ 1 - \frac{R}{R_0} + \frac{1}{2\pi} \sin\left(\frac{2\pi R}{R_0}\right) \right] \text{ ns}^{-1} \quad (3)$$

where  $\tau_3$  and  $R$  are expressed in the units of ns and Å, respectively.  $R_0$  equals  $R + \Delta R$ , where  $\Delta R$  is the fitted empirical electron layer thickness with a value of 1.66 Å. The relative fractional free volume (%), or the number of free volume content ( $f_v$ ), is expressed as follows<sup>20,21</sup>:

$$f_v = C \left( \frac{4\pi R^3}{3} \right) I_3 \quad (4)$$

where  $I_3$  (%) is the o-Ps intensity and  $C$  is a constant.

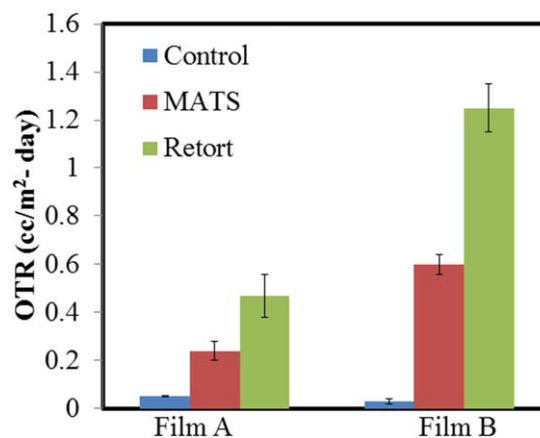


**Figure 2.** Oxygen transmission rate of films A and B, as influenced by the two thermal sterilization conditions. [Color figure can be viewed in the online issue, which is available at [wileyonlinelibrary.com](http://wileyonlinelibrary.com).]

### Data Analysis

A completely randomized design was used to evaluate the gas barrier and thermal properties for the films before and after processing. A general linear model was used to analyze the data, and Fisher's least significant difference test was used to determine significant differences ( $P < 0.05$ ) in film properties. Data analysis was conducted with statistical software, SAS version 9.2 (SAS Institute, Cary, NC).

## RESULTS AND DISCUSSION

### Film Characterization After Thermal Sterilization

This section discusses the gas barrier, morphological, and free volume changes in films A and B immediately after MATS and retort sterilization.

### Oxygen Transmission Rate

The OTR of the two films before (control) thermal treatment and immediately after MATS and retort sterilization is shown in Figure 2. Before thermal processing, the OTR of film A and film B were 0.04 and 0.03 cc/m<sup>2</sup> day, respectively. The barrier-coated film B had slightly better oxygen barrier properties than film A. Nevertheless, the two polymeric packaging materials used in this study had significantly lower OTRs compared with laminated polyvinylidene chloride barrier films or silicon oxide-coated films, which are currently used as lid films and flexible pouch materials in the retail market for thermally processed shelf-stable foods. These commercially available films have OTRs in the range of 0.3–2.3 cc/m<sup>2</sup> day.<sup>8</sup>

Both MATS and retort sterilization significantly increased ( $P < 0.05$ ) the OTR of films A and B immediately after processing. There was a sixfold and 12-fold increase in the OTR of film A after the MATS and retort processes, respectively. On the other hand, the OTR for film B increased 20 times after MATS processing, and increased by about 41 times after hot water retort treatment. That is, the OTR for films A and B after retort sterilization was twice that of MATS treatment for the same level of sterilization ( $F_0 = 6$  min). Therefore, the shorter overall processing time in MATS (nearly 9 min) compared with conventional retort (nearly 28 min) implies that packaging

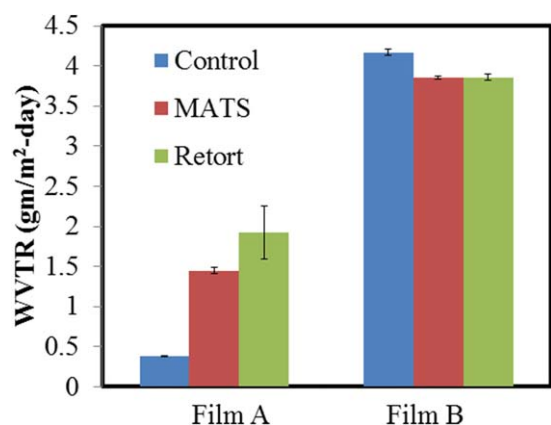


**Figure 3.** Water vapor transmission rate of films A and B, as influenced by the two thermal sterilization conditions. [Color figure can be viewed in the online issue, which is available at [wileyonlinelibrary.com](http://wileyonlinelibrary.com).]

materials deteriorate to a lesser degree after exposure to harsh processing conditions of heat and moisture. This could have a direct effect on oxygen barrier properties of packaging films.

Mokwena et al.<sup>8</sup> studied the effect of MW and retort sterilization on multilayer EVOH films used as lidstock films for rigid polymeric trays. They found that EVOH films exhibited more than twice the level of deterioration in OTR when processed with retort sterilization as compared to MW treatment. They attributed the higher deterioration level in OTR during retort sterilization to increased plasticization from water absorption by the hydrophilic EVOH layer during processing. They also found that longer processing time resulted in higher water absorption by the films. The hydrophilic nature of EVOH is one of the major reasons for their reduced desirability as packaging material in conventional thermal sterilization applications. However, because our study involved hydrophobic PET films as the functional barrier layer, the deterioration in oxygen barrier properties could be due to morphological and structural changes in the polymer during and after processing.

Even though films A and B had a statistically comparable OTR before thermal treatment, it is interesting to note that the increase in OTR of film B after MATS and retort sterilization was significantly greater than that of film A, which had no barrier coating in the PET layer (Figure 2). In particular, after the MATS treatment, the OTR of film B was 2.5 times higher than

that of film A. On the other hand, the ratio of OTR of film B to that of film A was 2.7 for the retort sterilization. The disparity in the performance of the two films may have been caused by differences in morphological and free volume properties of the individual polymer layers used in each multilayer film structure. The stability of the barrier coating layer present in film B during thermal sterilization may also affect oxygen barrier properties during thermal processing.

#### Water Vapor Transmission Rate

Figure 3 shows the WVTR of the two films before (control) thermal treatment and immediately after treatment by MATS and retort sterilization. The WVTR of the two films before processing (control) differed significantly ( $P < 0.05$ ), with nearly 11 times greater transmission in film B than in film A. However, after thermal sterilization by MATS and retort sterilization, the WVTR of film B remained statistically comparable, with no significant changes ( $P > 0.05$ ). On the other hand, film A showed a significant increase in WVTR after thermal sterilization, and retort sterilization treatment had a greater effect than did MATS. There was also a 3.8-fold and fivefold increase in the WVTR of film A after the MATS and retort processes, respectively. It is possible that the shorter processing time of MATS (nearly 9 min) compared with that of retort sterilization (nearly 28 min) caused less deterioration in the structural properties of film A, and hence, the higher water vapor barrier property.

#### Thermal Analysis

DSC analysis was used to determine the melting temperature ( $T_m$ ) and enthalpy of fusion/melting ( $\Delta H_m$ ) of the individual film components of film A and film B. The crystalline morphology of semi-crystalline materials can be characterized using the thermal parameters,  $T_m$  and  $\Delta H_m$ .<sup>22</sup> The crystallization mechanism influences the rate of gas transmission through food packaging films. The two thermal processes had no significant influence ( $P > 0.05$ ) on the melting temperature and enthalpy of melting of the different components of the film A and film B (Table I). Because the DSC study did not reveal any substantial impact of MATS and retort sterilization on the crystalline morphology of the individual polymer layers, the issue was further investigated with XRD analysis. This investigation will help establish the limitation of the DSC method in correlating the thermal sterilization conditions with the crystallinity of films A and B.

**Table I.** Melting Temperature and Enthalpy of Melting of the Individual Layers for the Films A and B, Untreated, and After Thermal Sterilization

Film <sup>a</sup>	Treatment	$T_m$ (°C)			$\Delta H$ (J/g)		
		PP	Nylon	PET	PP	Nylon	PET
A	Control	162.4 ± 0.1	219.8 ± 0.2	255.8 ± 0.1	20.3 ± 4.6	6.0 ± 1.3	3.6 ± 0.4
	Microwave	161.7 ± 1.3	219.5 ± 0.1	255.8 ± 0.1	19.2 ± 3.5	7.3 ± 0.1	5.2 ± 0.6
	Retort	162.3 ± 0.1	220.0 ± 0.4	256.2 ± 0.1	23.3 ± 3.3	7.8 ± 1.2	5.3 ± 0.5
B	Control	163.0 ± 0.2	220.0 ± 0.1	256.2 ± 0.1	33.5 ± 8.0	11.5 ± 5.3	5.0 ± 1.1
	Microwave	161.5 ± 0.1	218.9 ± 0.1	254.6 ± 0.2	33.7 ± 4.8	8.5 ± 0.9	4.7 ± 0.6
	Retort	161.6 ± 0.3	219.2 ± 0.2	254.6 ± 0.1	27.4 ± 0.3	8.6 ± 0.5	4.4 ± 0.8

<sup>a</sup>Film A: PET/adhesive/Nylon/adhesive/PP; Film B: Coated-PET-Coated/adhesive/oriented Nylon/adhesive/PP.

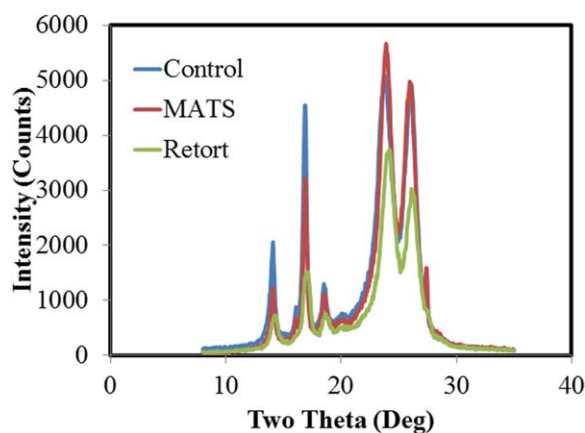


**Figure 4.** X-ray diffraction patterns for film A before and after the two thermal sterilization treatments. [Color figure can be viewed in the online issue, which is available at [wileyonlinelibrary.com](http://wileyonlinelibrary.com).]

### X-ray Diffraction

Figure 4 provides an illustration of the XRD patterns for film A before (control) and after the two sterilization treatments. The overall crystallinity of the polymeric films was measured by considering the area under the curve of the peaks for the measured scattering range. MATS treatment led to an increase in peak area and intensity in the scattering angle range above 20 degrees, which increased the overall crystallinity of film A from 64% to 69%. This increase in the crystallinity of film A suggests greater orderliness in the polymeric chains. Peaks above 20 degrees in film A correspond to that of Ny and PET, whereas PP could be characterized by the peaks below 20 degrees (Figure 4). The crystallinity of the PP peak at nearly 17 degrees decreased after thermal sterilization, whereas the crystallinity for Ny and PET increased. Thus, the increase in crystallinity of Ny at nearly 24 degrees and PET at nearly 26 degrees was responsible for the overall improvement of crystalline morphology of MATS processed film A.<sup>23,24</sup> On the other hand, the retort sterilization led to a slight decrease in overall crystalline region for film A. The longer processing time in retort sterilization compared with MATS likely led to the exposure of the polymeric film to a high-moisture environment, which could result in the plasticization of Ny, the hydrophilic polymer present in the film. This plasticization could cause distortion of some of the crystal structures of film A, and hence, the loss in crystallinity. The superior oxygen and water vapor barrier properties in film

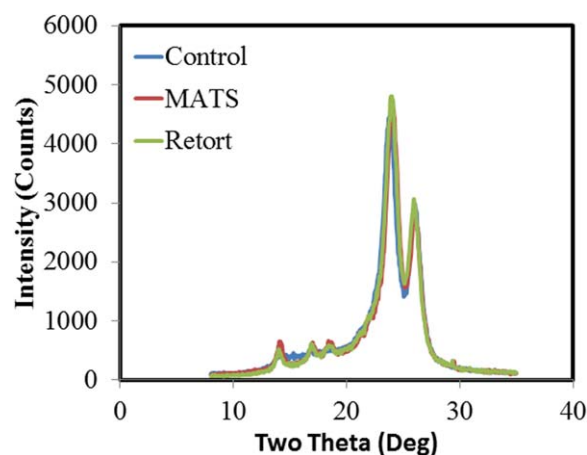


**Figure 5.** X-ray diffraction patterns for film B before and after the two thermal sterilization treatments. [Color figure can be viewed in the online issue, which is available at [wileyonlinelibrary.com](http://wileyonlinelibrary.com).]

A after MATS versus retort sterilization may be attributed to an increase in the tortuous path for the gas to travel through the film, resulting from the improved crystalline morphology of film A after MATS treatment.

Figure 5 provides an illustration of the XRD patterns for film B before (control) and after the two sterilization treatments. Film B also showed an increase in overall crystallinity from 59 to 62% after MATS, whereas crystallinity remained statistically comparable after retort sterilization. This improved crystalline morphology due to the Ny peak at 24 degrees could be responsible for the higher oxygen barrier property of film B after MATS, as compared with retort sterilization.<sup>24</sup> The crystallinity of the PP peak at nearly 17 degrees and PET at 26 degrees remained nearly the same after thermal sterilization. In addition, film B had lower levels of crystalline region compared with film A after the two sterilization treatments, which may have increased gas transmission through film B, despite the barrier coating present on its barrier PET layer. Furthermore, the disparity in the morphology of the individual polymer layers and the adhesive layers present in the two films manufactured by different companies could be responsible for the different gas barrier properties after sterilization treatment.

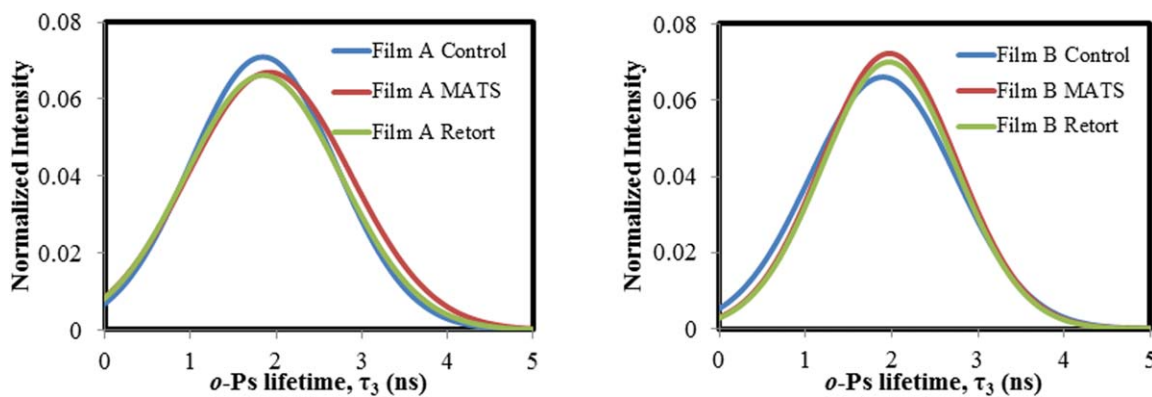
### Free Volume Analysis by PALS

Table II summarizes the effects of thermal sterilization treatment on the o-Ps parameters measured by PALS. The thermal

**Table II.** o-Ps Parameters from the Positron Annihilation Lifetime Spectroscopy Study for the Films A and B, Untreated, and After Thermal Sterilization

Film <sup>a</sup>	Treatment	o-Ps lifetime, $\tau_3$ (ns)	o-Ps intensity, $I_3$ (%)	Free volume radius ( $\text{\AA}$ )	Free volume fraction ( $F_v$ )
A	Control	1.84	15.19	2.70	2.25
	MW	1.92	15.91	2.78	2.58
	Retort	1.86	15.08	2.72	2.30
B	Control	1.89	14.00	2.75	2.20
	MW	1.97	14.21	2.82	2.40
	Retort	1.97	13.68	2.82	2.31

<sup>a</sup>Film A: PET/adhesive/Nylon/adhesive/PP; Film B: Coated-PET-Coated/adhesive/oriented Nylon/adhesive/PP.



**Figure 6.** o-Ps lifetime distribution of films A and B before and after the two thermal sterilization treatments. [Color figure can be viewed in the online issue, which is available at [wileyonlinelibrary.com](http://wileyonlinelibrary.com).]

treatment resulted in an increase in the o-Ps lifetime for the two films, which validates the increase in free volume size and fraction of the polymer matrix. The free volume fraction ( $F_v$ ) for film A increased by 15% after MATS and 2% after retort sterilization. On the other hand, film B exhibited a 9% increase in  $F_v$  after MATS treatment and a 5% increase after retort sterilization. This thermally induced increase in  $F_v$  could lead to the formation of transient-free volume gaps, which provide a low-resistance avenue for gas transmission through the polymer matrix. Additionally, Figure 6 shows changes in the o-Ps lifetime distribution for both films A and B after the MATS and retort treatment. Lifetime distribution of film B shows an increase in the normalized intensity after MATS and retort sterilization, whereas the intensity decreased for film A. This implies that thermal treatment induced a change in the motion of the polymer chains within the polymer matrix for the two films.<sup>11</sup> The increase in lifetime distribution for film B led to more free volume available for gas to transmit through its polymeric matrix and could be responsible for the relative increase in OTR and WVTR of film B being greater than that of film A.

The increase in  $F_v$  for the two films after MATS compared with retort sterilization can be attributed to the different heating mechanism used in MATS (Table II). The volumetric MW heating of MATS versus conventional retort sterilization may lead to higher localized temperatures in the polymeric films. These temperature increases lead to formation of thermally induced free volume gaps. It should be noted that the overall film crystallinity after MATS treatment was higher than with retort sterilization. Thus, the level of amorphous and crystalline region in the two polymeric films varied. This could influence the level of changes in film morphology and gas-barrier properties. Thus, synthesizing results from free volume studies and crystalline morphology helped us to understand the deterioration of oxygen barrier properties for the two films after thermal sterilization.

## CONCLUSIONS

In this study, we found that MATS and retort sterilization caused a significant deterioration in oxygen barrier properties of films A and B. The level of deterioration was significantly higher after retort sterilization compared with MATS treatment. These

results may be explained by the reduced changes in morphological properties of polymeric packaging materials after the MATS process with a shorter overall processing time compared with conventional retort. XRD revealed up to 5% improvement in crystalline morphology of MW treated films in terms of overall crystallinity as compared with retort sterilization. PALS studies revealed an increase in the normalized intensity in Film B after thermal sterilization which helps to explain the relative increase in OTR and WVTR of film B being greater than that of film A. This was the first study to apply PALS in MATS-treated polymeric materials. Combining PALS and XRD can reveal the influence of free volume characteristics and film morphology on gas-barrier properties of MATS and retort-processed high barrier multilayer polymeric films. Findings suggest that flexible plastic pouches containing PET as the barrier layer are a suitable packaging material for the processing shelf-stable foods using MATS application.

## ACKNOWLEDGMENTS

This work was funded in part by the Food Security USDA Special Research Grants # 2008–34477–09142 and # 2009–34477–20304, as well as by USDA NIFA Research Grant # 2011–68003–20096. PALS measurements were funded in part by National Science Foundation Grant # DMR 1006772. The authors thank Robert Armstrong and Masakazu Nakaya of EVAL Company of America, as well as Jim Lamb of Alcan Packaging for providing the packaging materials for testing. They also acknowledge the technical assistance of Feng Liu and Zhongwei Tang of Washington State University.

## REFERENCES

- Dhawan, S.; Barbosa-Cánovas, G. V.; Tang, J.; Sablani, S. S. *J. Appl. Polym. Sci.* **2011**, *122*, 1538.
- Morris, C. E. *Food Eng. Mag.* **1996**, *3*, 73.
- Brody, A. L. *Food Technol.* **2012**, *66*, 78.
- Guan, D.; Plotka, V. C. F.; Clark, S.; Tang, J. *J. Food Process. Pres.* **2002**, *26*, 307.
- Ramaswamy, H.; Tang, J. *Food Sci. Technol. Int.* **2008**, *14*, 423.

6. Tang, J.; Liu, F.; Patfiak, K.; Eves, E. E. *U.S. Pat.* 7,119,313 B2 (2006).
7. Bermúdez-Aguirre, D.; Barbosa-Cánovas, G. V. *Food Eng. Rev.* **2011**, 3, 44.
8. Mokwena, K. K.; Tang, J.; Dunne, C. P.; Yang, T. C. S.; Chow, E. J. *Food Eng.* **2009**, 92, 291.
9. Yoo, S.; Lee, J.; Holloman, C.; Pascall, M. A. *J. Appl. Polym. Sci.* **2009**, 112, 107.
10. Awad, S.; Chen, H. M.; Brian, P. G.; Paul, A.; Ford, W. T.; Lee, L. J.; Jean, Y. C. *Macromolecules* **2012**, 45, 933.
11. Wang, Z. F.; Wang, B.; Qi, N.; Zhang, H. F.; Zhang, L. Q. *Polymer* **2005**, 46, 719.
12. Dhawan, S.; Varney, C.; Barbosa-Cánovas, G. V.; Tang, J.; Selim, F.; Sablani, S. S. *J. Food Eng.* **2014**, 128, 40.
13. Pandit, R. B.; Tang, J.; Liu, F.; Mikhaylenko, G. *Pattern Recognit.* **2007**, 40, 3667.
14. Downing, D. L. *A Complete Course in Canning and Related Processes: Book II*, 13th ed.; CTI Publications, Inc.: Baltimore, MD, **1996**.
15. American Society for Testing and Materials [ASTM]. Standard Test Method for Oxygen Gas Transmission Rate Through Plastic Film and Sheeting Using a Coulometric Sensor. ASTM Book of Standards, D3985-95; American Society for Testing and Materials: Philadelphia, PA, **1995**.
16. American Society for Testing and Materials [ASTM]. Standard Test Method for Water Vapor Transmission Rate Through Plastic Film and Sheeting Using a Modulated Infrared Sensor. ASTM Book of Standards, F1249; American Society for Testing and Materials, Philadelphia, PA, **1990**.
17. Jean, Y. J. *Mater. Sci. Forum* **1994**, 175, 59.
18. Selim, F. A.; Varney, C. R.; Rowe, M. C.; Collins, G. S. *Phys. Rev. Lett.*, submitted.
19. Kansy, J. *Nucl. Instrum. Methods Phys. Res. Sect. A* **1996**, 374, 235.
20. Cheng, M. L.; Sun, Y. M.; Chen, H.; Jean, Y. C. *Polymer* **2009**, 50, 1957.
21. Ramya, P.; Ranganathaiah, C.; Williams, J. F. *Polymer* **2012**, 53, 842.
22. Kong, Y.; Hay, J. N. *Eur. Polym. J.* **2003**, 39, 1721.
23. Karagiannidis, P. G.; Stergiou, A. C.; Karayannidis, G. P. *Eur. Polym. J.* **2008**, 44, 1475.
24. Rabiej, S.; Ostrowska-Gumkowska, B.; Wlochowicz, A. *Eur. Polym. J.* **1997**, 33, 1031.